Journal Pre-proof

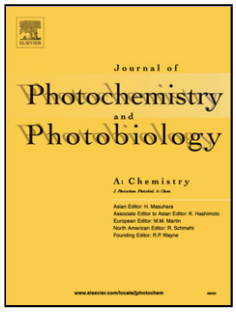

A novel “OFF–ON–OFF” fluorescence chemosensor for hypersensitive detection and bioimaging of Al(null) in living organisms and natural water environment

Chun Kan (Supervision), Xiaotao Shao (Conceptualization) (Methodology) (Software) (Data curation)<ce:contributor-role>Writing- original draft)<ce:contributor-role>Writing- review and editing), Linyun Wu (Visualization) (Investigation), Yao Zhang (Software), Xiaofeng Bao (Validation), Jing Zhu (Supervision)

PII: S1010-6030(20)30417-2

DOI: https://doi.org/10.1016/j.jphotochem.2020.112618

Reference: JPC 112618

To appear in: *Journal of Photochemistry & Photobiology, A: Chemistry*

Received Date: 10 February 2020

Revised Date: 22 April 2020

Accepted Date: 6 May 2020

Please cite this article as: Kan C, Shao X, Wu L, Zhang Y, Bao X, Zhu J, A novel “OFF–ON–OFF” fluorescence chemosensor for hypersensitive detection and bioimaging of Al(x2162;) in living organisms and natural water environment, *Journal of Photochemistry & Photobiology, A: Chemistry* (2020), doi: https://doi.org/10.1016/j.jphotochem.2020.112618

A novel "OFF–ON–OFF" fluorescence chemosensor for hypersensitive detection and bioimaging of Al(Ⅲ) in living organisms and natural water environment

Chun Kan [a, 1, *], Xiaotao Shao [a, 1], Linyun Wu [a], Yao Zhang [a], Xiaofeng Bao [b], Jing Zhu [c, *]

[a] College of Science, Department of Chemistry and Material Science, Nanjing Forestry University, 159 LongpanRoad, Nanjing 210037, PR China
[b] School of Environmental and Biological Engineering, Jiangsu Key Laboratory of Chemical Pollution Control and Resources Reuse, Nanjing University of Science and Technology, Nanjing 210094, China
[c] Department of Pharmacy, Jiangsu Key Laboratory for Pharmacology and Safety Evaluation of Chinese Materia Medica, Nanjing University of Chinese Medicine, 138 XianlinDadao, Nanjing 210023, China

[*]Corresponding author, Email address: kanchun@njfu.edu.cn (Chun Kan).
[1]These authors contributed equally to this work.

Highlights

- A new hypersensitive Al^{3+} probe based on rhodamine B was developed.
- The probe can be considered as a reversible fluorescent switch to detect Al^{3+} with 1:1 binding stoichiometry.
- The probe can respond immediately to Al^{3+}, which is reflected in the instantaneous change of solution color and fluorescence.
- The detection limit of this probe is as low as 14.23nM.
- The probe has been successfully applied to image Al^{3+} in living cells, animal and plant tissues.
- The probe has been proved to work properly in natural water.

Abstract

High-selectivity detection of trace Al^{3+} ions in water and biological systems by a fluorescence imaging method is not yet mature. Herein, we synthesized a novel reversible Al^{3+}-specific fluorescent probe named RBLF by linking Rhodamine B and pyridine-3-sulfonyl chloride through o-phenylenediamine in several reactions. RBLF exhibited an ultra-high sensitive and excellent selective response towards Al^{3+} by fluorescence and UV-visible spectra in aqueous solutions. What is more worth mentioning is that its response is fast, dual changes in color and fluorescence of the

probe solution that can occur instantaneously after adding with Al^{3+}. Its detection limit for Al^{3+} ions in aqueous system solutions is 14.23 nM, which is far below the maximum allowable amount of Al^{3+} in drinking water. Moreover, the probe provided an effective method for detecting low concentrations of Al^{3+} in natural water, living cells, zebrafish and plant tissues.

Keywords: Hypersensitive fluorescent probe; Aluminum (Ⅲ) detection; Reversibility; Natural water; Biological application

1. Introduction

As the third most abundant element in the earth's crust and the first most abundant in metallic elements, aluminum is widely found in nature and the biosphere in the form of silicate, bauxite and ion. At present, the progress and development of various industries seem to be inseparable from aluminum, because of its excellent physical and chemical properties, these also laid its status as the second category of metals. Aluminum is often used in industrial production and daily life, such as water purification, food additives, cosmetics and medicine, etc. [1]. This makes it easier for aluminum to contact directly with living organisms, which may lead to environmental degradation or accumulation of aluminum in the body [2]. However, aluminum is not an essential metal element for human body, nor is it a trace element. When the content of Al^{3+} in human body accumulates to a certain degree, it will produce toxicity harmful to human. In 2017, aluminum was included in the list of carcinogens by the World Health Organization's International Agency for Research on Cancer. Because human brain tissue has affinity for Al^{3+}, a large amount of Al^{3+} can destroy the human central nervous system and immune system, cause erythrocyte hypochromic anemia, inhibit the activity of a variety of enzymes in the body and accelerate human aging. In terms of disease, Alzheimer disease [3-5]and ParKinson Diseautomotive service engineers [6-9] can be induced; a large amount of Al^{3+} can also affect the ingestion and utilization of essential microelements needed by human body, thereby increasing the risk of breast cancer in women [10]. For animals and plants, when the content of Al^{3+} reaches a certain level, the soil will become acidified, which is not conducive to the growth of plant roots and seeds [11, 12]. When lakes, rivers and oceans contain excessive amounts of Al^{3+}, the growth and development of various aquatic fish will be inhibited, causing fish die due to lack of essential nutrients [13]. The World Health Organization (WHO) states that the weekly intake of Al^{3+} by human should be less than 7 mg per kilogram [14]. Therefore, it is crucial to design a highly selective and sensitive method for detecting the content of Al^{3+} in order to reduce its damage to the body and ecology.

Prior to the advent of new analytical methods, there have been several traditional methods to detect aluminium ion. The widely used detection technology mainly includes Inductively coupled plasma optical emission spectroscopy (ICP-OES), Inductively coupled plasma mass spectrometry (ICP-MS), Graphite furnace atomic absorption spectrometry (GF-AAS), Atomic fluorescence spectrometry (AFS) and chromatography [15-19]. Although these analysis methods have the advantages of high

accuracy and good stability, the shortcomings such as high use and maintenance costs, complicated equipment debugging, and poor convenience have greatly limited their wide application. In recent years, fluorescence analysis has developed rapidly and become a new research hotspot [20, 21]. Compared with traditional high sensitivity methods, the fluorescence analysis method has the advantages of low cost, easy operation, repeatability and diversity of detection materials. Fluorescence sensor is the most typical method of fluorescence analysis. Moreover, fluorescent sensors have obvious advantages over other methods in ion monitoring of living cells and biological tissues, because of their nondestructive properties, instantaneous responsiveness and indicator dye diversity [22-25]. Fluorescent sensors are mostly a class of compounds derived from fluorescent groups such as Rhodamine[26-29], coumarin [30-32], pyrene [33, 34] and naphthalene [35, 36]. Among them, Rhodamine is favored by researchers for its excellent photostability, high fluorescence quantum yield, high molar extinction coefficient, unique switching mechanism [17], low toxicity and other outstanding photophysical properties, and has gradually developed into a popular fluorescent group [37]. Most rhodamine-based fluorescent sensors work by opening and closing the spiral ring. At first, the helix ring was in a closed loop state without fluorescence generation; under the action of ion complexation, the rhodamine lactam spiral ring structure is broken, and the ring opens and emits fluorescence [38, 39].

In this paper, we designed and synthesized an Al^{3+} hypersensitive fluorescence sensor called RBLF with rhodamine B as the fluorophore. Firstly, rhodamine B reacts with phosphorus oxychloride to get its acyl chloride, which makes it easier to react with o-phenylenediamine later. We modified the probe (N-TC) synthesized in our previous work and replaced the original linking group with o-phenylenediamine that has a rigid structure and a strong planar conjugate effect [40]. The amino group is an electron-donor group, which will greatly enhance the fluorescence effect and sensitivity of probe. However, pyridine-3-sulfonyl chloride with good ion coordination ability was still retained as the recognition group, and the final probe RBLF was obtained (scheme 1).

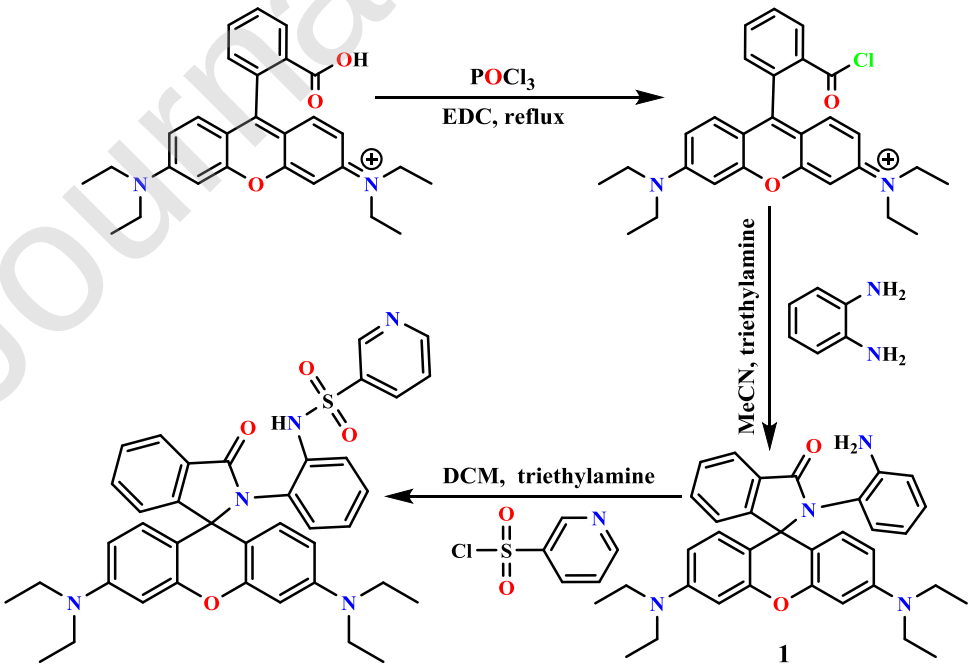

Scheme 1. Synthesis of RBLF

2. Experimental

2.1. Reagents and instrumentation

Unless specifically stated, none of the solvents and chemical reagents purchased from Aladdin (Shanghai, China) require further purification. The water used in the whole experiment was ultrapure water. The silica gel GF254 plate used for TLC analysis and the silica gel used for chromatography column were all purchased from Haiyang Chemical Co., Ltd. (Qingdao, China). Metal ion stock solution was prepared in advance with nitrate or chloride corresponding to the metal.

An Avance III HD 600MHz fully digital superconducting nuclear magnetic resonance spectrometer was used to record NMR spectra with $CDCl_3$ as solvent and tetramethylsilane (TMS) as the internal standard. The fluorescence spectra and the UV–Vis absorption spectra were performed by an Edinburgh FLS920 fluorescence spectrophotometer and a Shimadzu UV-3600 UV–vis-NIR spectrophotometer respectively. Electrospray ionization mass spectra (ESI-MS) were acquired with a Thermo-Fisher Scientific dual-focus high resolution instrument under electron ionization conditions. Bioimaging were implemented with a laser confocal microscopy (ZEISS, LSM710) and inverted fluorescence microscope (OLYMPUS, IX81).

2.2. Synthesis of compound 1

Rhodamine B (960 mg, 2 mmol) was stirred and dissolved in anhydrous dichloroethane at a round bottom flask of 50 mL. $POCl_3$ (1 mL, 11 mmol) was slowly added under the atmosphere of N_2, and then the system was reflux for 6h. After the reaction, the solvent and excess $POCl_3$ were removed by decompression to obtain the purple oily acyl chloride. The purple oil obtained previously was redissolved in 40 mL acetonitrile, o-phenylenediamine (432 mg, 2 mmol) dissolved in 10 mL acetonitrile and triethylamine (1 mL, 7.2 mmol) was added in drops. The reaction process was monitored by TLC after overnight stirring at room temperature. When the reaction was completed, decompress to remove the solvent. The crude products were extracted three times with dichloromethane and saturated NaCl solution, and then extracted once with reversed-phase. The organic phase was dried, filtered, and concentrated by vacuum distillation to obtain compound 1(787.8 mg, 74%). ^{1}H NMR (600 MHz, $CDCl_3$), δ 8.03(d, J=7.26 Hz, 1H), 7.56(m, 2H), 7.25(dd, J_1=6.18 Hz, J_2=1.5 Hz, 1H), 6.95(m, 1H), 6.64(s, 2H), 6.65(d, J=7.92 Hz 1H), 6.40(t, J=7.5 Hz, 1H), 6.27(t, J=33.72 Hz 4H), 6.08(d, J=7.14 Hz, 1H), 3.32(s, 8H), 1.63(m, 1H), 1.14(t, J=6.9 Hz, 12H) ppm. ^{13}C NMR(126 MHz, $CDCl_3$), δ 166.50, 154.01, 152.32, 148.90, 144.54, 134.68, 132.67,131.97, 128.91, 128.73, 128.41, 124.33, 123.46, 122.12, 120.32, 118.23, 116.98, 116.81, 108.04, 98.10, 68.13,45.81, 45.20, 44.43, 12.60, 12.52, 8.62 ppm.

2.3. Synthesis of RBLF

Compound 1 (532 mg, 1 mmol) was dissolved in an appropriate amount of dichloromethane, pyridine-3-sulfonyl chloride (179.04μL, 1.5 mmol) and triethylamine

(138.99 μL, 1 mmol) were added and stirred at room temperature for 6 h. The progress of the reaction was monitored by chromatography. After the reaction, the solvent was evaporated under reduced pressure. The compound was rapidly separated by silica gel column with CH_2Cl_2/Ethyl Acetate (9:1, v/v) used as an eluent. A pale pink solid (342.4 mg, 51%) was obtained as the fluorescence sensor RBLF towards Al^{3+}. ^1H NMR (600 MHz, $CDCl_3$), δ 8.99(d, J=1.74 Hz 1H), 8.76(dd, J_1=4.74 Hz, J_2=1.2 Hz, 1H), 7.99(t, J=10.38 Hz 2H), 7.62(m, 2H), 7.38(m, 1H), 7.32(d, J=7.32 1H), 7.25(d, J=8.04 Hz, 1H), 7.10(m, 1H), 6.79(m, 1H), 6.62(t, J=8.88 3H), 6.44(d, J=7.56 2H), 6.27(s, 2H), 6.21(dd, J_1=7.92 Hz, J_2=1.2 Hz, 1H), 3.36(m, 8H), 1.67(s, 1H), 1.18(t J=7.02 Hz 12H) ppm. ^{13}C NMR(126 MHz, $CDCl_3$), δ 168.08, 153.95, 153.22, 151.49, 149.31, 148.07, 136.71,134.97, 134.82, 133.26, 131.47, 130.27, 129.01, 128.82, 128.07, 126.91, 124.80, 124.51, 123.79, 123.60, 120.43, 108.84, 105.93, 98.03, 68.85, 53.45, 44.49, 31.44, 30.21, 29.70, 12.48 ppm. ESI-MS m/z: calculated for $C_{39}H_{39}N_5O_4S$: 673.2723, $[M+H]^+$ found, 674.2804; $[M+Na]^+$ found, 696.2626.

2.4. Preparation for spectral experiments

The stock solutions of cationic (5mM) including Al^{3+}, Ag^+, Cr^{3+}, Ca^{2+}, Cd^{2+}, Co^{2+}, Fe^{2+}, Fe^{3+}, Li^+, K^+, Mn^{2+}, Mg^{2+}, Ni^+, Na^+, Zn^{2+} and Pb^{2+} were respectively prepared. Some common anions including $H_2PO_4^-$, Br^-, BrO_3^-, $B_4O_7^{2-}$, I^-, NO_3^-, SO_4^{2-}, $S_2O_8^{2-}$ and IO_3^- are also configured as solutions in the same way as before. The stock solution of RBLF was prepared at 5mM with the solution of EtOH/H_2O (1:2, v/v). The excitation wavelength for spectral experiments was selected at 520nm, and the emission wavelength was selected from 530nm to 700nm. In addition, the reversibility of RBLF was determined by fluorescence spectrometry and UV–Vis absorption spectrometry with fluoride ion solution. To verify whether RBLF can respond in the real environment, we examined its performance in natural water. In addition to that, we adjusted the pH of the system to around 7.3 before testing, which simulated the physiological pH environment, and completed the test as soon as possible.

2.5. Cytotoxicity and cell imaging studies

The incubation conditions and methods of the cells, as well as the specific procedures of toxicity test and cell imaging, were described in the supporting materials.

2.6. Zebrafish and plant imaging

Detailed information about zebrafish and the processing of biometric imaging are described in the supplementary materials.

3. Results and discussion

3.1. Spectral response of probe toward metal ions and anions

For the sake of determining which ions can be detected by RBLF, several common metal ions including Ag^{+}, Al^{3+}, Ca^{2+}, Cd^{2+}, Co^{2+}, Cr^{3+}, Fe^{2+}, Fe^{3+}, K^{+}, Li^{+}, Mg^{2+}, Mn^{2+}, Na^{+}, Ni^{+}, Pb^{2+} and Zn^{2+} were selected for fluorescence spectrum and UV-Vis absorption spectrum test in EtOH/H_2O (1:2, v/v) solution containing 10μM RBLF. The specificity of probe is the primary factor to test whether the probe has good performance. Fluorescence spectrum test results showed that the intensity of the solution increased significantly only when added Al^{3+}. Although the addition of Fe^{2+} produced a slight fluorescence enhancement effect higher than other ions, it was negligible compared to Al^{3+}. The addition of other ions had little effect on the fluorescence intensity of the solution originally containing only RBLF (Fig. 1). In addition, the solution added with Al^{3+} became pink visible to the naked eye, while the other solutions remained colorless and transparent. RBLF itself has no absorption peak at 500-600nm. Only after adding Al^{3+}, obvious absorption peak also appeared in the UV-Vis absorption spectrum (Fig. S6).

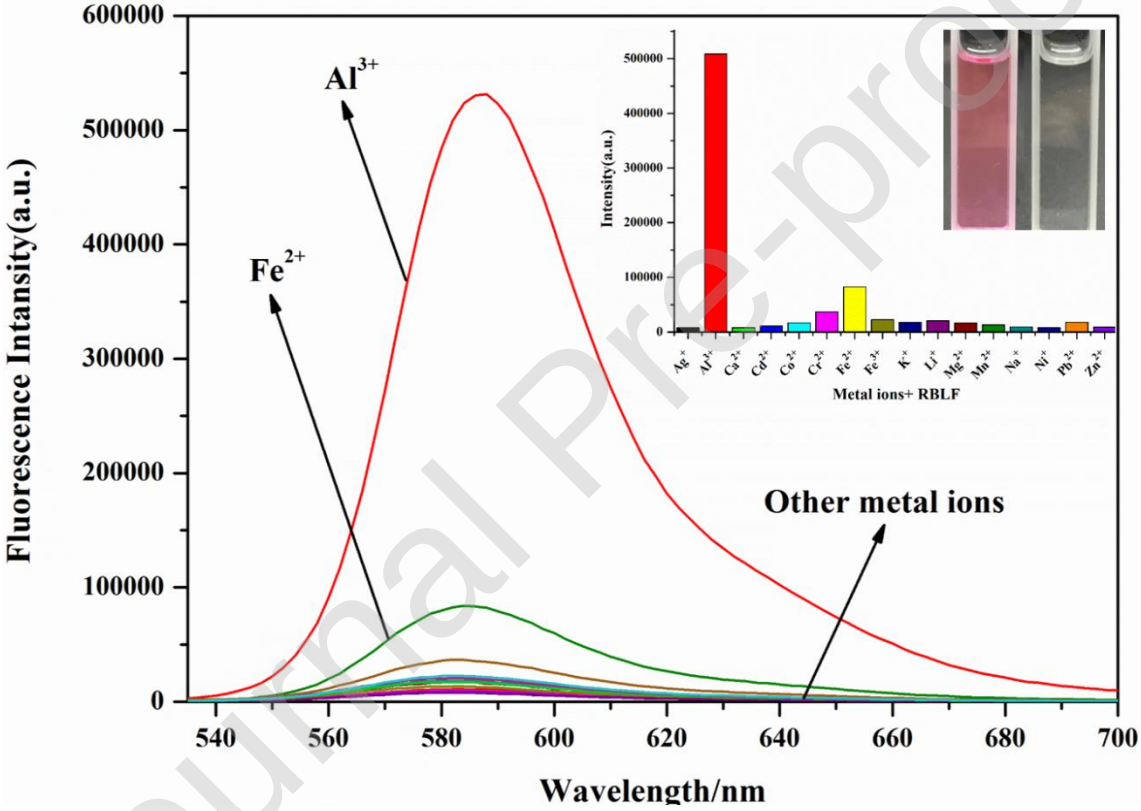

Fig. 1. (A) Fluorescence spectra of RBLF (10 μM) in a EtOH/H_2O (1:2, v/v) solution with the existence of various metal ions. The inset in (A) represents the fluorescence intensity ($\lambda_{ex=}$ 520nm, λ_{em}=582nm) of RBLF in the presence of various metal ions.

We also designed a set of competitive experiments to verify whether RBLF can accurately detect Al^{3+} in this environment when other metal ions are present, so as to evaluate the specificity of RBLF to Al^{3+}. As shown in Fig. 2, the fluorescence intensity of solutions containing RBLF and other measured metal ions increased sharply after the addition of Al^{3+}, which was close to or even more than that of the probe solution

in presence of only Al^{3+}. This indicated that other metal ions have no negative impact on the specificity of RBLF for detecting Al^{3+}, which indirectly indicates that RBLF has higher selectivity.

In the normal working environment of the probe, there must be not only metal ions, but also other anions. Therefore, we designed an experiment to test the interference of several anions during RBLF operation. We added $H_2PO_4^-$, Br^-, BrO_3^-, $B_4O_7^{2-}$, I^-, NO_3^-, SO_4^{2-}, $S_2O_8^{2-}$ and IO_3^- respectively to the solution containing Al^{3+} and RBLF. Excitingly, even with the addition of the above anions, the fluorescence intensity of the original solution did not decrease. This showed that even in complex ionic environment RBLF can also efficiently detect Al^{3+}, which provides the possibility to detect Al^{3+} in natural water environment (Fig. S7).

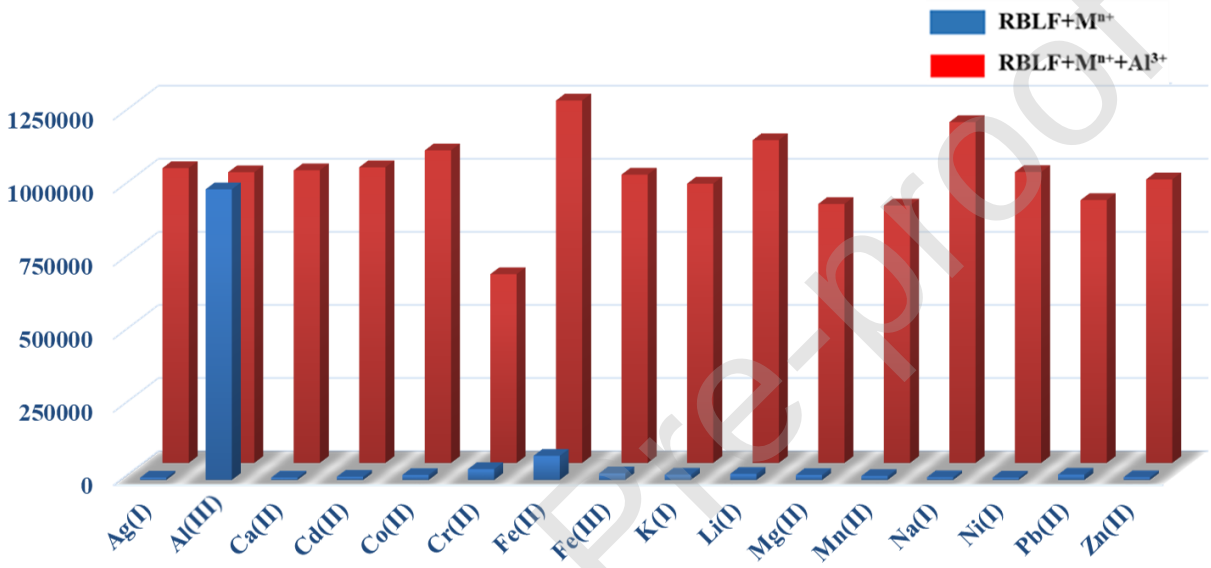

Fig. 2. Comparison of fluorescence intensity of probe solutions containing different metal ions (10 μM) before and after adding Al^{3+} in EtOH/H_2O solution (1:2, v/v). Blue bars: RBLF added with several common cations. Red bars: add Al^{3+} to above mixed solutions.

3.2. Response of RBLF to pH value and time

The spiral ring of rhodamine compounds are sensitive to pH. When the pH value of the environment is very low, spironolactone is destroyed to produce a strong fluorescence, which may be a potential interference factor, so the pH titration experiment is very necessary. As can be seen from Fig. S8, when pH < 6, RBLF had a distinct fluorescent signal, but gradually decreased. When pH is between 6 and 12, RBLF has almost no fluorescence. For RBLF-Al^{3+}, when pH value was less than 8, the fluorescence intensity was strong and stable. When pH > 8, fluorescence intensity began to decline drastically. The above test results showed that the RBLF fluorescence signal is weak at physiological pH, which provides a good fluorescence background for biological imaging of RBLF. However, RBLF-Al^{3+} had a strong fluorescence intensity,

indicating that bioimaging is achievable.

The response time of the probe is also an important criterion to evaluate its performance, so we explored the response time of RBLF. 60μL of Al^{3+} was added to the probe system solution prepared in advance, and then the fluorescence intensity was tested every 20s. As shown in Fig. 3, the fluorescence intensity increased significantly after the addition of Al^{3+}. The rising speed was obviously accelerated between 80s and 180s, but gradually slowed down after 180s, and the fluorescence intensity reached its maximum and became stable after 240s. Therefore, RBLF can be viewed as a hypersensitive probe for Al^{3+}. All the above experiments were conducted in EtOH/H_2O (1:2, v/v) solution.

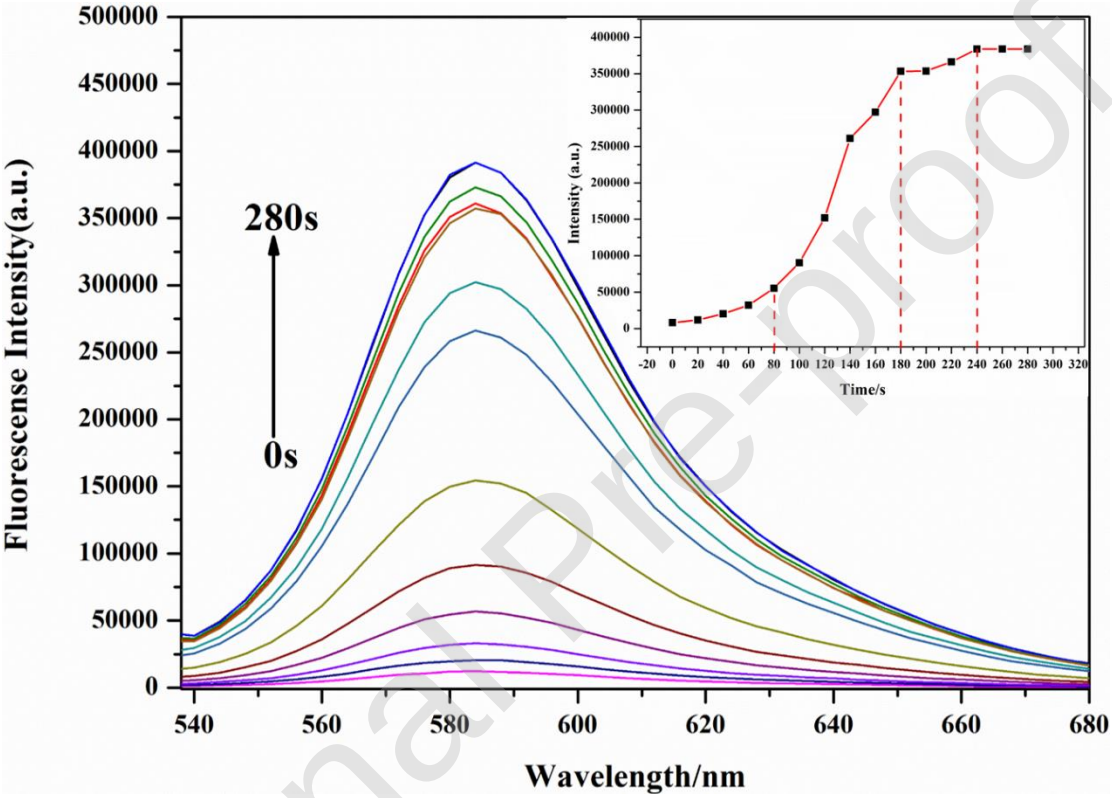

Fig. 3. Fluorescence spectra of RBLF (10 μM) with Al^{3+} in the EtOH/H_2O (1:2, v/v) solution. The excitation wavelengths were 520 nm and the wavelengths of emission were 582 nm. Inset: Plot of the fluorescence intensities at 582 nm during a period of 280s.

3.3. Sensitive quantification of RBLF to Al^{3+}

To further explore the sensing properties of the probe along with the interaction between RBLF and Al^{3+}, a fluorescence titration experiment were performed. According to the fluorescence titration experiment results (Fig. 4), when Al^{3+} was slowly added dropwise in EtOH/H_2O (1:2, v/v) solution containing RBLF, the fluorescence intensity of the mixed solution began to rise slowly, and the color of the solution turned pink. When 1.2 equivalents of Al^{3+} were added, the fluorescence intensity increased rapidly and the color of the solution deepened. After adding 10

equivalent of Al^{3+}, the rising speed of fluorescence intensity slowed down, and the fluorescence intensity tended to be stable after adding 20 equivalent of Al^{3+}. Therefore, RBLF responded to the increase concentration of Al^{3+} with fluorescence intensity and color.

In order to further explore the binding mechanism of RBLF and Al^{3+}, we calculated the binding constant of RBLF, which is a key factor, according to the Benesi-Hildebrand formula ($F-F_0=\Delta F= [Al^{3+}] (F_{max}-F_0)/(1/K_a+[Al^{3+}])$based on the titration experiment results. The binding constant is calculated by linearly fitting the independent variable $1/[Al^{3+}]$ with the dependent variable $1/(F_{max}-F_0)$. Where F_0 is the initial fluorescence intensity of probe RBLF, F is the fluorescence intensity of RBLF after adding a certain amount of Al^{3+}, and F_{max} is the fluorescence intensity when Al^{3+} is excessive. From this linear relationship (Fig. S9A), the concentration range of Al^{3+} in the unknown solution can be roughly determined. In addition, the binding constant can be calculated as$1.16\times10^4\ M^{-1}$.

The detection limit is also a key component of probe performance. In the beginning, we measured the fluorescence spectroscopy of standard solution containing RBLF only every 5 min for a total of 10 times, and calculated the standard deviation of fluorescence intensity with the fluorescence value at 582 nm (Fig. S9B). Then, according to the formula DL=3SD/S, the detection limit of RBLF for Al^{3+} was calculated to be 14.23nM, which was far lower than the maximum of 7μM in drinking water stipulated by the World Health Organization.

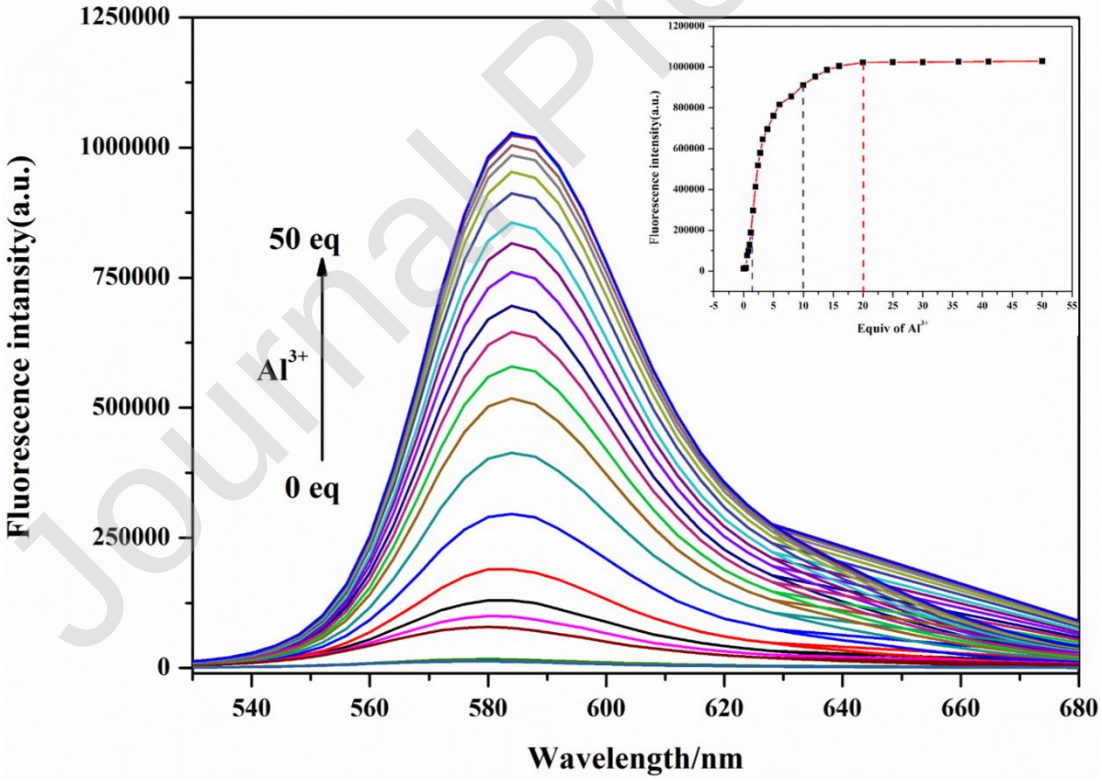

Fig. 4. Different concentrations of Al^{3+} (0–50 equiv.) was added in EtOH/H_2O (1:2, v/v) solutions containing RBLF (10 μM). Inset: Fluorescence intensities plot of mixed solution at 582 nm with gradually increased addition of Al^{3+}.

3.4. Stoichiometry and sensing mechanism of RBLF

In order to further study the stoichiometry of RBLF and Al^{3+}, the Job's plot curve was drawn to confirm the complexation ratio of ions and target compounds in the liquid phase. In this work, the coordination ratio between RBLF and Al^{3+} was determined by reference to the fluorescence spectrum. The total concentration of RBLF and Al^{3+} remained at 50 μM, and the Al^{3+} content ratio ranged from 0 to1. The concentration of Al^{3+} is accounted for as a function of the fluorescence intensity of the solution at 582 nm. As can be seen from the Fig. 5, when the mole fraction of Al^{3+} was 0.5, the fluorescence intensity was the maximum, indicating that RBLF and Al^{3+} are 1:1 ratio. On the basis of above experimental results, a reasonable sensing mechanism of RBLF was proposed (Scheme 2).

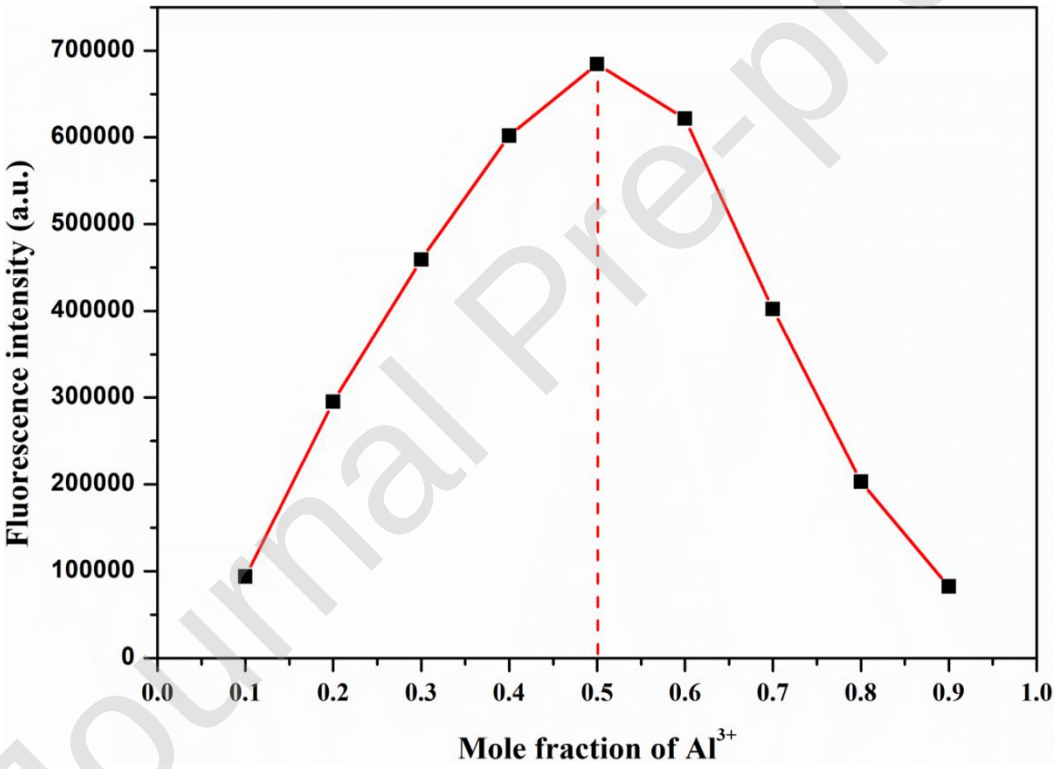

Fig. 5. Job's plot to determine the stoichiometry between RBLF and Al^{3+} ([RBLF]+[Al^{3+}]=50 μM) in EtOH/H_2O (1:2, v/v) solution at 582 nm.

Reversibility is a common characteristic of rhodamine-based probes for practical application, and the reversibility of RBLF was studied below. As shown in the Fig. 6, a constant amount of Al^{3+} and F^- were added alternately and repeatedly in the solution of RBLF to make a switchable fluorescence intensity change at 582nm, and the operation could be repeated indefinitely by adding $Al^{3+}$and F^- successively. Therefore, the original

RBLF had fluorescence enhanced response to Al^{3+}, which could be reversed by adding F^-. In other words, the original RBLF is the specific probe of Al^{3+}, while RBLF-Al^{3+} can work as a probe for F^-. This is mainly because fluorine and aluminum ions are anions and cations, and they will form chemical bonds. The difference in electronegativity between aluminum and fluorine atoms is greater than 1.7, so they may form ionic bonds. Or they form complexes that reduce the coordination between Al^{3+} and RBLF.

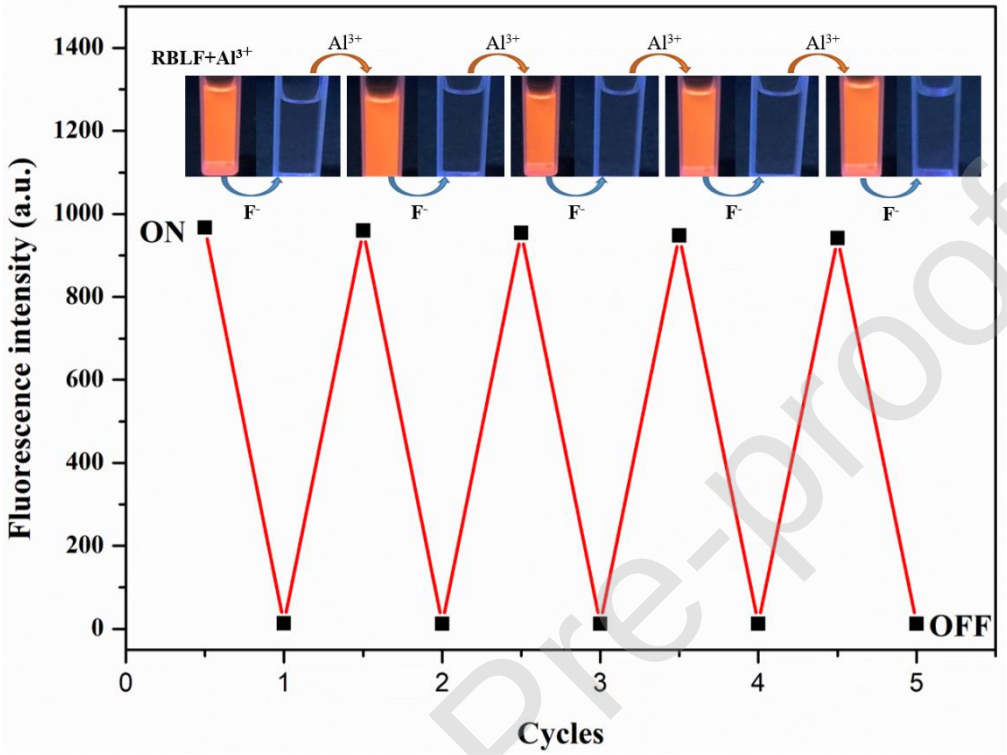

Fig. 6. Fluorescent intensity of RBLF (10μM) at 582 nm in the solution of EtOH/H_2O (1:2, v/v) upon the alternate addition of Al^{3+} (1 equiv.) and F^- (2 equiv.). Images of fluorescence reversibility under 365 nm UV lamp.

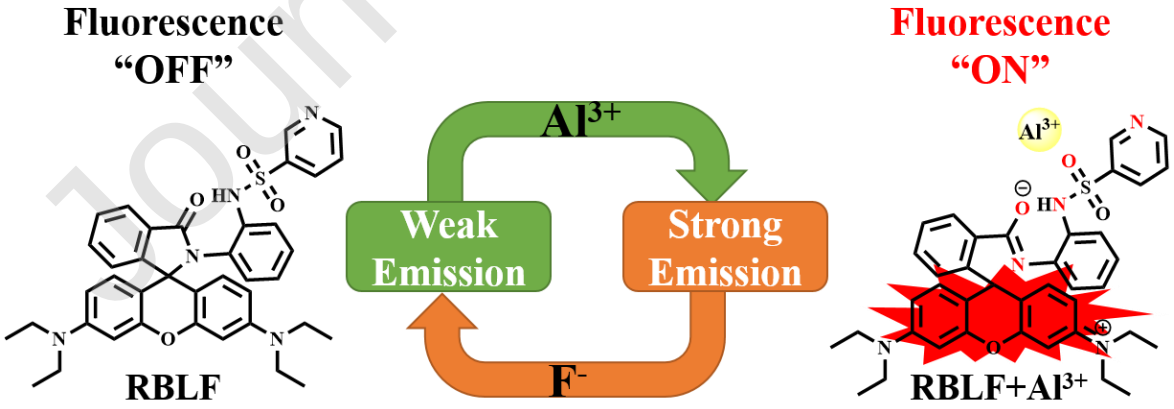

Scheme 2. Proposed sensing mechanism of RBLF towards Al^{3+}

To further elucidate the proposed sensing mechanism or the property of the complexation between RBLF and Al^{3+}, ^1H NMR titration of RBLF was performed in the absence or existence of Al^{3+} in DMSO-d_6 solution (Fig. 7). As seen in the ^1H NMR spectra of free RBLF, the aromatic proton peak is strong and sharp. After the addition of Al^{3+}, the chemical shift of several peaks have changed, especially the H_q peak on the pyridine ring. Its chemical shift was originally around δ 7.85 ppm. After adding Al^{3+}, the peak became weaker and wider, and the proton signal upfield shifted to around δ 7.80 ppm. This indicated that the N on the pyridine ring also participated in the coordination of Al^{3+}. Additionally, upon the addition of Al^{3+}, a new strong peak appeared at δ 5.7-5.8ppm, which is the active hydrogen of N in rhodamine spironolactone, indicating that spironolactone transforms into an open-loop amide and complexed with Al^{3+}.

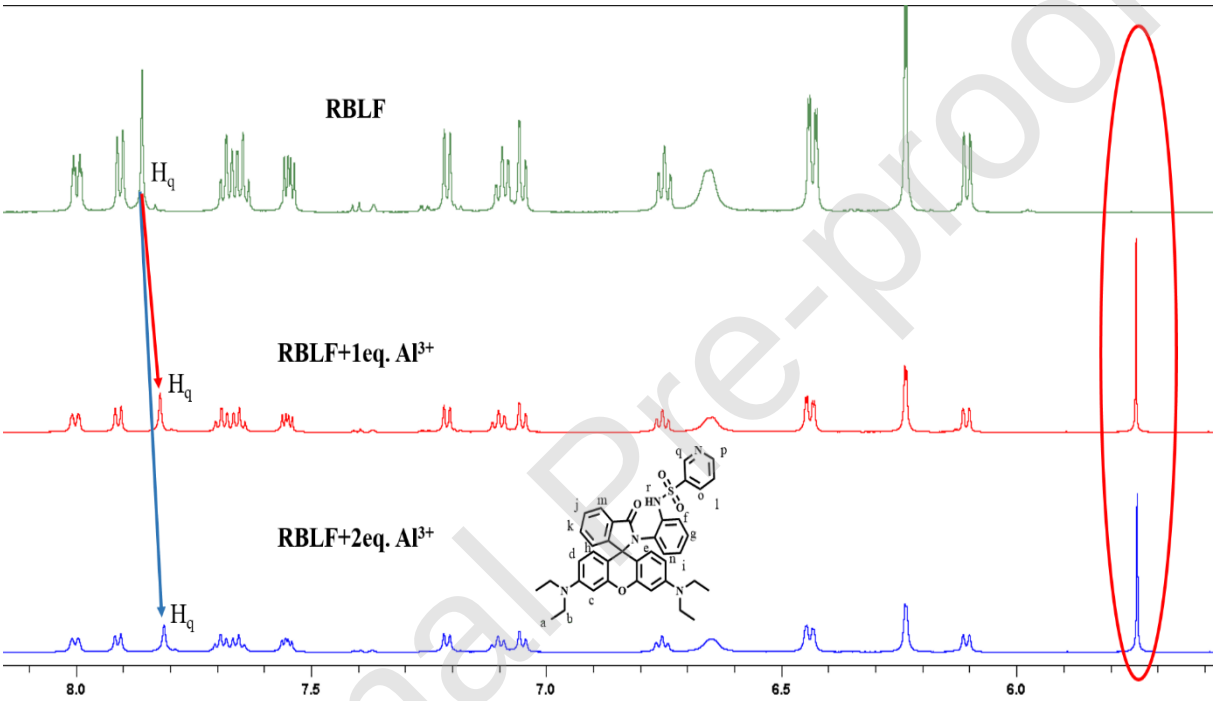

Fig. 7. Partial spectra of ^1H NMR titration of RBLF with Al^{3+} in DMSO-d_6

3.5. Study on detection of Al^{3+} by RBLF in natural water

In order to explore whether the probe RBLF can detect trace Al^{3+} well in the natural water environment which is much more complicated than the test environment, we collected two local river and lake water samples (Xuanwu Lake and Zihu Creek)for experiment. All the water samples were filtered for removing excess Al^{3+}. After that, different amount of Al^{3+} were spiked within the samples. As can be seen from the Table 1, the recovery of Al^{3+} in natural water ranges from 89.6% to 99.0%. It is obvious that even in real water samples where impurities and ions may interfere with the complexation of RBLF with Al^{3+} and affect the fluorescence intensity, the recovery is still good. Thus, the above experiments showed that RBLF could be used to detect Al^{3+} in the real environment.

3.6. Cytotoxicity and detection of intracellular Al^{3+}

For further evaluating the bioavailability and value in intracellular Al^{3+} bioimaging of the synthesized probe RBLF, we conducted a living cell fluorescence imaging experiment. Firstly, MTT assay was used to study the cytotoxicity, and the possibility of its application in cells was preliminarily verified. As can be seen From the Fig. S10, even when the concentration of RBLF in the environment reaches 20 μM, the survival rate of MCF-7 cells can be maintained more than 85%. As expected, RBLF has lower toxicity and is fully capable of working well in cells. Next, we designed fluorescence experiments to observe the intracellular imaging of RBLF. We used blue channels to track living cells, and divided the cells into three groups, which were incubated with Al^{3+}, RBLF, and the both. We used blue channels to mark cells and observed cell imaging through bright fields, blue channels, fluorescent channels, and superimposed channels. As shown in the Fig. 8, cells incubated with Al^{3+} alone did not produce fluorescence. When the cells were incubated with RBLF alone for a few hours, weak fluorescence began to appear in the cells. After adding 10μM of Al^{3+} for co-incubation for a period of time, the cells maintained normal activity and morphology, and a wide range of intense fluorescence appeared in the cells. The above results indicated that RBLF had low biotoxicity and good biocompatibility. Ensure that it can detect Al^{3+} normally in cells without affecting cell survival and reproduction.

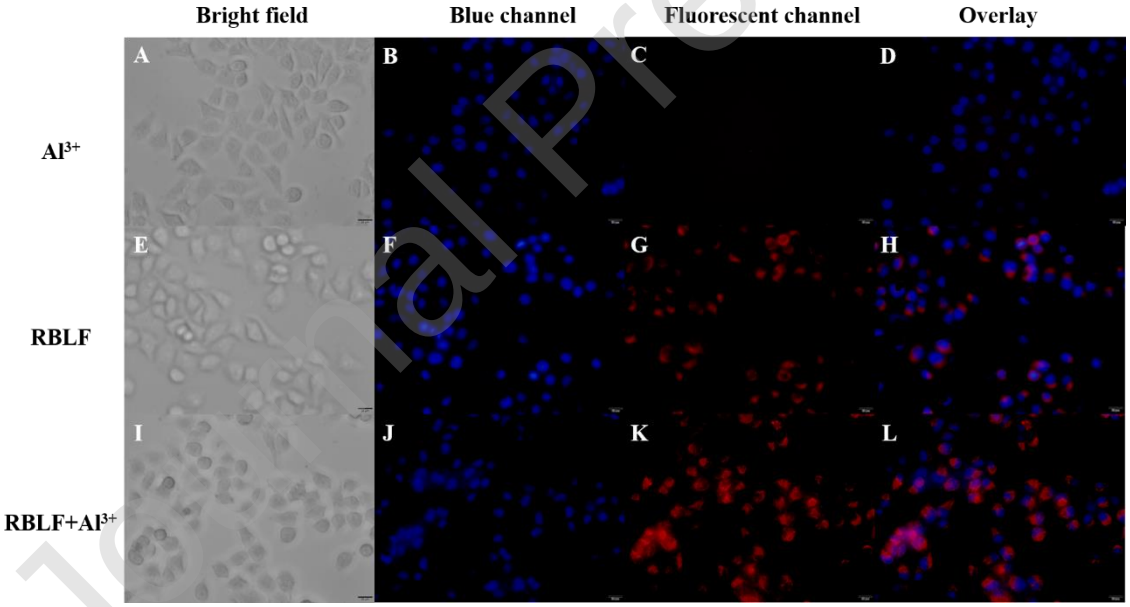

Fig. 8. LSCM (laser scanning confocal microscopy) images of RBLF in living MCF-7 cells. (A-D): Cells with only treatment; (E-F): Cells treated with only RBLF (10 μM); (I-L): Cells co-treated with RBLF and Al^{3+} (10 μM). (A, E, I) Bright field; (B, F, J) Blue channel (λ_{ex} = 340 nm, monitored at 420-480 nm); (C, G, K) Fluorescent channel (λ_{ex}= 550 nm, λ_{em} = 560-680 nm); (D, H, L) Overlay channel. Conditions: 5% CO_2/95% air atmosphere at 37 ℃.

3.7. Fluorescence microscope images of living organisms

In addition to the above mentioned cell imaging, we also attempted to apply RBLF to detect trace aluminum ions in living organisms. We selected zebrafish with high transparency, small size and soybean sprout tissue with high water content, good imaging effect for experiment. As shown in Fig. 9, almost no fluorescence was observed in the zebrafish incubated in an aqueous solution containing only RBLF (A-C). After 30 min of incubation with Al^{3+}, the fish began to show fluorescence in the body. Especially in the fish's internal organs and tissue fluids, the fluorescence was more pronounced, forming the outline of the entire zebrafish (D-F). Similarly, soybean sprouts grown in an environment that contained Al^{3+} showed no fluorescence, compared to a group of beans grown in an Al^{3+} solution that were immersed in a probe solution for another 30 min and produced an incredibly bright red fluorescence (Fig. 10). The above results indicate that RBLF, with its high sensitivity and biocompatibility, can effectively detect trace amounts of Al^{3+} in living organisms, showing great development prospects in biological detection.

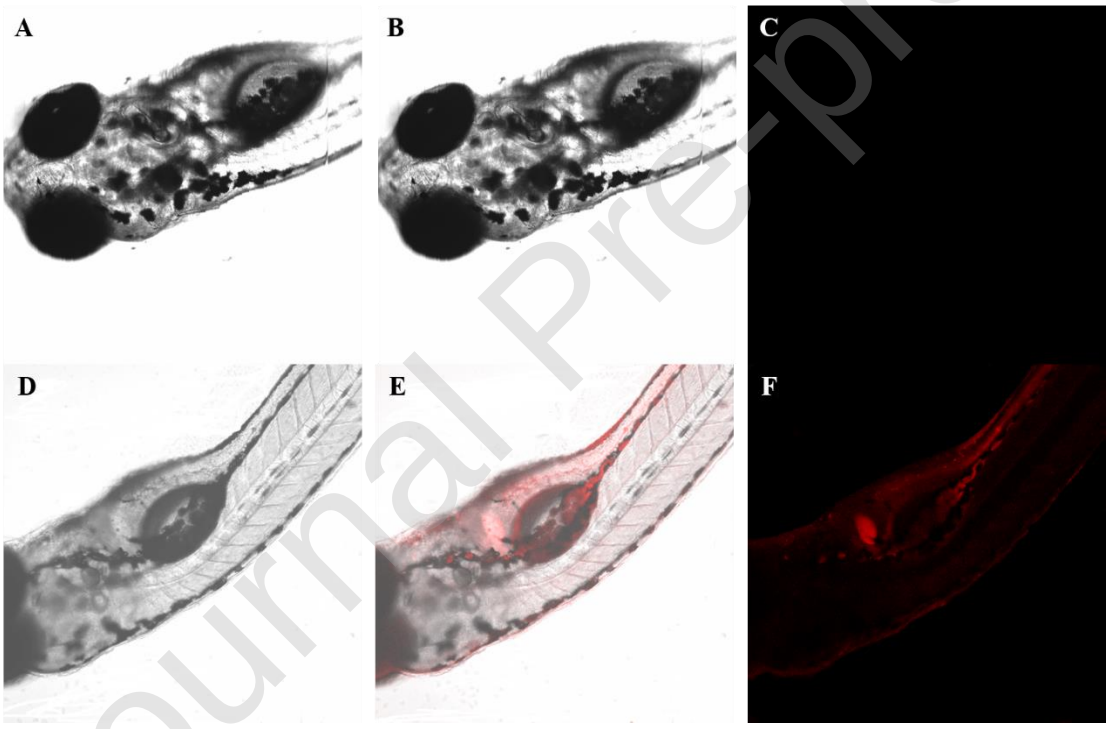

Fig. 9. LSCM images of zebrafish (λ_{ex}=543nm). Zebrafish were incubated for 30 min in a solution of only RBLF (10μM) (A-C). Zebrafish firstly cultured for 30 min with RBLF and then fed with Al^{3+} (10 μM) (D-F). (A, D) Bright field, (B, E) Mixed images, (C, F) Fluorescent images. Conditions: 100% air atmosphere at 25 ℃.

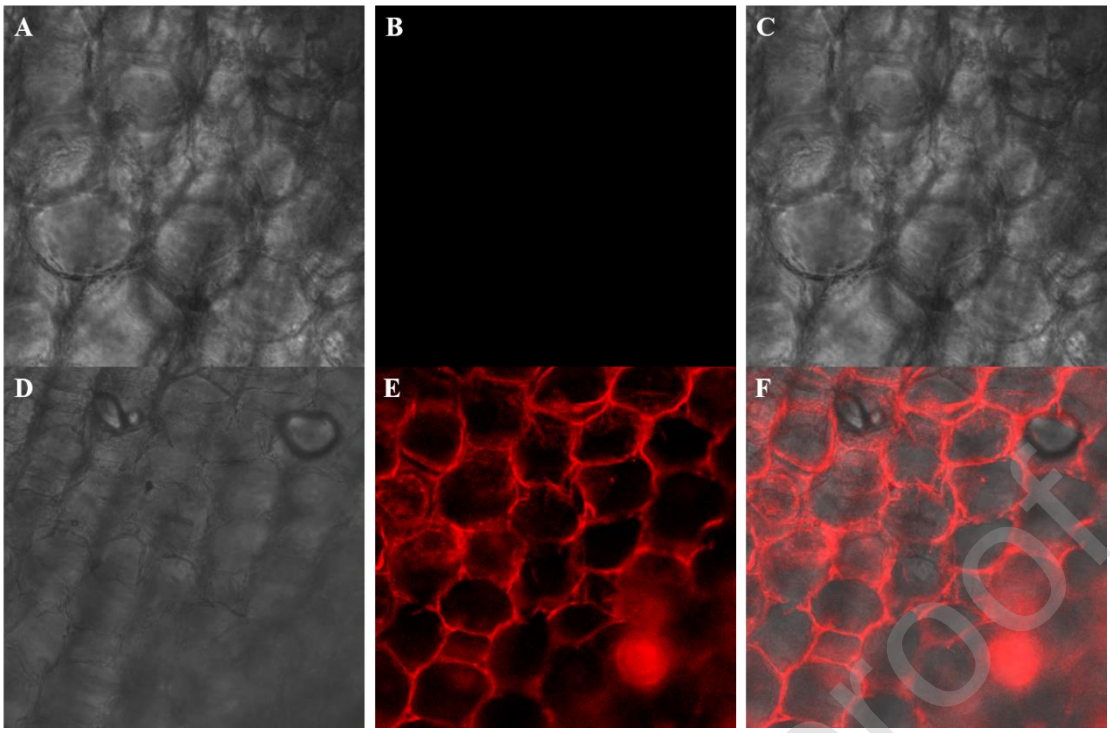

Fig. 10. LSCM images of soybean sprouts root tissues (λ_{ex}=543nm). Soybean raised in the environment with only RBLF (10μM) (A-C). Soybean germinated in the environment with only Al^{3+} (10μM) and also treated with RBLF (10μM) for 30 min (D-F). (A, D) Bright field, (B, E) Fluorescent images, (C, F) Mixed images. Conditions: 100% air atmosphere at 25 ℃.

4. Conclusion

In summary, an Al^{3+} hypersensitive fluorescent probe RBLF based on rhodamine B was synthesized and characterized. It can be regarded as a naked-eye probe, which produces fluorescence effect and color change immediately after adding Al^{3+}. RBLF exhibits high selectivity and high sensitivity for Al^{3+}, it has a lower detection limit of 14.23nM and a shorter response time of only 280s. In addition, RBLF-Al^{3+} can realize an "OFF-ON" fluorescence response through adding F^-, the solution also become colorless gradually. RBLF-Al^{3+} has a good selectivity to F^-, which can be thought as a fluorescence probe. Furthermore, RBLF has been successfully used to detect trace amounts of Al^{3+} in natural water, living cells, zebrafish and plant tissues on the basis of its good water solubility and low toxicity.

Declaration of Interest Statement

We declare that we have no financial and personal relationships with other people or organizations that can inappropriately influence our work, there is no professional or other personal interest of any nature or kind in any product, service and/or company that could be construed as influencing the position presented in, or the review of, the manuscript entitled.

Author statement

Chun Kan and Jing Zhu: Supervision.

Xiaotao Shao: Conceptualization, Methodology, Software, Data curation, Writing- Original draft preparation, Writing- Reviewing and Editing.

Linyun Wu: Visualization, Investigation.

Yao Zhang: Software

Xiaofeng Bao: Validation.

Acknowledgements

The authors express their gratitude to Jiangsu Six Talent Peak Award (2015SWYY013) and The Priority Academic Program Development of Jiangsu Higher Education Institutions (PAPD), which provided financial supports. We also gratefully and sincerely acknowledge the technical along with equipment supports from Advanced analysis and testing center of Nanjing Forestry University.

References

[1] Z. Liu, H. Xu, L. Sheng, S. Chen, D. Huang, J. Liu, A highly selective colorimetric and fluorescent chemosensor for Al(III) based-on simple naphthol in aqueous solution, Spectrochim. Acta A 157 (2016) 6-10.

[2] A. Ghorai, J. Mondal, S. Chowdhury, G.K. Patra, Solvent-dependent fluorescent-colorimetric probe for dual monitoring of Al^{3+} and Cu^{2+} in aqueous solution: an application to bio-imaging, Dalton T. 45 (2016) 11540-11553.

[3] L. Azib, N. Debbache-Benaida, G. Da Costa, D. Atmani-Kilani, N. Saidene, K. Ayouni, T. Richard, D. Atmani, Pistacia lentiscus L. leaves extract and its major phenolic compounds reverse aluminium-induced neurotoxicity in mice, Ind. Crop. Prod. 137 (2019) 576-584.

[4] A.A. Ali, H.I. Ahmed, S.A. Khaleel, K. Abu-Elfotuh, Vinpocetine mitigates

aluminum-induced cognitive impairment in socially isolated rats, Physiol. Behav. 208 (2019) 9.

[5] H.N. Mustafa, Neuro-amelioration of cinnamaldehyde in aluminum-induced Alzheimer's disease rat model, J. Histotechnol. (2019) 1-10.

[6] B. Mitrovica, R. MilaEiEa, B. Pihlar, Speciation of Aluminium in Soil Extracts by Employing Cation-exchange Fast Protein Liquid Chromatography-Inductively Coupled Plasma Atomic Emission Spectrometry, Analyst. 121 (1996) 627-634.

[7] D.R.C. McLachlan, C. Bergeron, P.N. Alexandrov, W.J. Walsh, A.I. Pogue, M.E. Percy, T.P.A. Kruck, Z.D. Fang, N.M. Sharfman, V. Jaber, Y.H. Zhao, W.H. Li, W.J. Lukiw, Aluminum in Neurological and Neurodegenerative Disease, Mol. Neurobiol. 56 (2019) 1531-1538.

[8] W. Laabbar, A. Elgot, O. Elhiba, H. Gamrani, Curcumin prevents the midbrain dopaminergic innervations and locomotor performance deficiencies resulting from chronic aluminum exposure in rat, J. Chem. Neuroanat. 100 (2019) 101654-101654.

[9] W.J. Lukiw, T.P.A. Kruck, M.E. Percy, A.I. Pogue, P.N. Alexandrov, W.J. Walsh, N.M. Sharfman, V.R. Jaber, Y. Zhao, W. Li, C. Bergeron, F. Culicchia, Z. Fang, D.R.C. McLachlan, Aluminum in neurological disease - a 36 year multicenter study, J. Alzheimer's Dis. 8 (2018).

[10] P.D. Darbre, Aluminium, antiperspirants and breast cancer, J. Inorg. Biochem. 99 (2005) 1912-1919.

[11] M.N. Alvim, F.T. Ramos, D.C. Oliveira, R.M.S. Isaias, M.G.C. Franca, Aluminium localization and toxicity symptoms related to root growth inhibition in rice (Oryza sativa L.) seedlings, J. Biosci. 37 (2012) 1079-1088.

[12] E. Delhaize, P.R. Ryan, Aluminum Toxicity and Tolerance in Plants, Plant Physiol. 107 (1995) 315-321.

[13] R.W. Gensemer, R.C. Playle, The bioavailability and toxicity of aluminum in aquatic environments, Crit. Rev. Environ. Sci. Technol. 29 (1999) 315-450.

[14] K. Boonkitpatarakul, J.-F. Wang, N. Niamnont, B. Liu, L. Mcdonald,Y. Pang, M. Sukwattanasinitt, Novel Turn-On Fluorescent Sensors with Mega Stokes Shifts for Dual Detection of Al^{3+} and Zn^{2+}, ACS Sensors 1 (2016) 144-150.

[15] A.B.S. Cabezuelo, M.M. Bayón, E.B. González, J.I.G. Alonso, A. Sanz-Medel, Speciation of basal aluminium in human serum by fast protein liquid chromatography with inductively coupled plasma mass spectrometric detection, Analyst 123 (1998) 865-869.

[16] J.W. Dilleen, B.J. Birch, B.G.D. Haggett, Electrochemical detection of aluminium using single-use sensors, Anal. Commun. 36 (1999) 363-365.

[17] I. Narin, M. Tuzen, M. Soylak, Aluminium determination in environmental samples by graphite furnace atomic absorption spectrometry after solid phase extraction on Amberlite XAD-1180/pyrocatechol violet chelating resin, Talanta 63 (2004) 411-418.

[18] S. Chen, Y.M. Fang, Q. Xiao, J. Li, S.B. Li, H.J. Chen, J.J. Sun, H.H. Yang, Rapid visual detection of aluminium ion using citrate capped gold nanoparticles, Analyst 137 (2012) 2021-2023.

[19] V.N. Mehta, R.K. Singhal, S.K. Kailasa, A molecular assembly of piperidine carboxylic acid dithiocarbamate on gold nanoparticles for the selective and sensitive detection of Al^{3+} ion in water samples, Rsc Adv. 5 (2015) 33468-33477.

[20] S. Das, M. Dutta, D. Das, Fluorescent probes for selective determination of trace level Al^{3+}: recent developments and future prospects, Anal. Methods 5 (2013).

[21] B.J. Pang, C.R. Li, Z.Y. Yang, Design of a colorimetric and turn-on fluorescent probe for the detection of Al(III), J. Photoch. Photobio. A 356 (2018) 159-165.

[22] A. Banerjee, A. Sahana, S. Das, S. Lohar, S. Guha, B. Sarkar, S.K. Mukhopadhyay, A.K. Mukherjee, D. Das, A naphthalene exciplex based Al^{3+} selective on-type fluorescent probe for living cells at the physiological pH range: experimental and computational studies, Analyst 137 (2012) 2166-2175.

[23] T.Y. Zhou, L.P. Lin, M.C. Rong, Y.Q. Jiang, X. Chen, Silver-gold alloy nanoclusters as a fluorescence-enhanced probe for aluminum ion sensing, Anal. Chem. 85 (2013) 9839-9844.

[24] M. Shellaiah, Y.H. Wu, H.C. Lin, Simple pyridyl-salicylimine-based fluorescence "turn-on" sensors for distinct detections of Zn^{2+}, Al^{3+} and OH^- ions in mixed aqueous media, Analyst 138 (2013) 2931-2942.

[25] S. Gui, Y. Huang, F. Hu, Y. Jin, G. Zhang, L. Yan, D. Zhang, R. Zhao, Fluorescence turn-on chemosensor for highly selective and sensitive detection and bioimaging of Al(3+) in living cells based on ion-induced aggregation, Anal. Chem. 87 (2015) 1470-1474.

[26] J. Mandal, P. Ghorai, K. Pal, T. Bhaumik, P. Karmakar, A. Saha, Development of Rhodamine 6G-Based Fluorescent Chemosensors for Al^{3+}-Ion Detection: Effect of Ring Strain and Substituent inEnhancing Its Sensing Performance, ACS Omega 5 (2020) 145−157.

[27] H.-S. Kim, S. Angupillai, Y.-A. Son, A dual chemosensor for both Cu^{2+} and Al^{3+}: A potential Cu^{2+} and Al^{3+} switched YES logic function with an INHIBIT logic gate and a novel solid sensor for detection and extraction of Al^{3+} ions from aqueous solution, Sens. Actuators B 222 (2016) 447-458.

[28] L. He, C. Liu, J.H. Xin, A novel turn-on colorimetric and fluorescent sensor for Fe^{3+} and Al^{3+} with solvent-dependent binding properties and its sequential response to carbonate, Sens. Actuators B 213 (2015) 181-187.

[29] K.-P. Wang, W.-J. Zheng, Y. Lei, S.-J. Zhang, Q. Zhang, S. Chen, Z.-Q. Hu, A thiophene-rhodamine dyad as fluorescence probe for ferric ion and its application in living cells imaging, J. Fluoresc. 208 (2019) 468-474.

[30] P.N. Borase, P.B. Thale, S.K. Sahoo, G.S. Shankarling, An “off–on” colorimetric chemosensor for selective detection of Al^{3+}, Cr^{3+} and Fe^{3+}: Its application in molecular logic gate, Sens. Actuators B 215 (2015) 451-458.

[31] Q. Sun, W.B. Zhang, J.H. Qian, A ratiometric fluorescence probe for selective detection of sulfite and its application in realistic samples, Talanta 162 (2017) 107-113.

[32] Z.X. Liu, X. Zhou, Y. Miao, Y. Hu, N. Kwon, X. Wu, J. Yoon, A Reversible

Fluorescent Probe for Real-Time Quantitative Monitoring of Cellular Glutathione Angew. Chem. 58 (2019) 6126-6126.

[33] S. Jang, P. Thirupathi, L.N. Neupane, J. Seong, H. Lee, W.I. Lee, K.-H. Lee, Highly Sensitive Ratiometric Fluorescent Chemosensor for Silver Ion and Silver Nanoparticles in Aqueous Solution, Org. Lett. 14 (2012) 4746-4749.

[34] X. Sun, Y.-W. Wang, Y. Peng, A Selective and Ratiometric Bifunctional Fluorescent Probe for Al^{3+} Ion and Proton, Org. Lett. 14 (2012) 3420-3423.

[35] X.X. Zhang, R.J. Wang, C.B. Fan, G. Liu, S.Z. Pu, A highly selective fluorescent sensor for Cd^{2+} based on a new diarylethene with a 1,8-naphthyridine unit, Dyes Pigments 139 (2017) 208-217.

[36] M.M. Yu, R.L. Yuan, C.X. Shi, W. Zhou, L.H. Wei, Z.X. Li, 1,8-Naphthyridine and 8-hydroxyquinoline modified Rhodamine B derivatives: "Turn-on" fluorescent and colorimetric sensors for Al^{3+} and Cu^{2+}, Dyes Pigments 99 (2013) 887-894.

[37] M. Tian, H. He, B.-B. Wang, X. Wang, Y. Liu, F.-L. Jiang, A reaction-based turn-on fluorescent sensor for the detection of Cu (II) with excellent sensitivity and selectivity: Synthesis, DFT calculations, kinetics and application in real water samples, Dyes Pigments 165 (2019) 383-390.

[38] C. Lim, H. Seo, J.-H. Choi, K.-S. Kim, A. Helal, H.-S. Kim, Highly selective fluorescent probe for switch-on Al^{3+} detection and switch-off F^{-} detection, J. Photoch. Photobio. A 356 (2018) 312-320.

[39] C.-Y. Li, Y. Zhou, Y.-F. Li, C.-X. Zou, X.-F. Kong, Efficient FRET-based colorimetric and ratiometric fluorescent chemosensor for Al^{3+} in living cells, Sens. Actuators B 186 (2013) 360-366.

[40] F. Song, X.T. Shao, J. Zhu, X.F. Bao, L. Du, C. Kan, Reversible “turn-off-on” fluorescence response of Fe(III) towards Rhodamine B based probe in vivo and plant tissues, Tetrahedron Lett. 60 (2019) 1363-1369.

Table 1. Results for the determination of Al^{3+} in water sample

Sample	Al^{3+} added (μM)	Detected (μM)	Recovery (%)
Xuanwu Lake	3	2.69 ± 0.03	89.6
	6	5.94 ± 0.09	99.0
	9	8.67 ± 0.17	96.3
	12	11.65 ± 0.09	97.1
	15	14.01 ± 0.22	93.7
	18	16.61 ± 0.18	92.3
Zihu Creek	3	2.78 ± 0.04	92.5
	6	5.69 ± 0.09	94.9
	9	8.86 ± 0.07	98.4
	12	11.70 ± 0.11	97.5
	15	14.37 ± 0.13	95.8
	18	16.24 ± 0.06	90.2